Elastoplastic nonlocal damage model for concrete and size effect analysis

A. Krayani, F. Dufour & G. Pijaudier-Cabot
ERT R&DO, GeM, Ecole Centrale de Nantes, France

ABSTRACT: This work deals with a combination of plasticity and nonlocal damage formulation for modelling concrete structure behaviour subjected to mixed mode failure. Plastic effect, driven by effective stress, is an hardening process and accounts for the development of irreversible strains while softening is controlled by damage to describe the degradation of the material stiffness. A regularization technique, based on the implicit gradient definition of the nonlocal strain tensor, is introduced to overcome the deficiencies induced by the softening damage relation i.e., spurious strain localization and dependance of the energy dissipation on mesh refinement. A 3D tensile bar localization benchmark is used to validate the effectiveness of the regularization technique. Moreover, simulation of reinforced concrete continuous deep beam is studied to illustrate the improvements achieved by coupled law compared to scalar damage models. Finally, size effect in mixed mode failure is investigated by mean of three asymmetric four-point bending tests on notched specimens.

1 INTRODUCTION

One of the specific behaviours of cementitious materials is that in uniaxial loading the traction strength is much smaller than compression strength. From that consideration, Mazars (1984) has developed a damage model which takes only the positive principal strains into account. This criterion is widely used for its simplicity and relative accuracy to represent mode I failures of concrete structures under monotone loading especially.

For some specific structures (thick and/or prestressed) the stress state may be locally bi- or tri-axial. As for any geomaterials the confinement has a positive effect on the structural strength and depending on the level of confinement the failure mode may change to mode II. For this reason, the modified von Mises criterion (de Vree et al. 1995) seems to be more attracive as the second invariant of the stress tensor is introduced into the yield criterion. However, this criterion is symetric (traction-compression) and does not represent the reality.

The idea followed by Jason et al. (2006) is to couple plasticity, based on the effective stress, and local damage formulation in one single constitutive relation in order to represent a correct volumetric response of concrete, i.e. the confinement effect and the non symetric response of the material. The damage process, controlled by elastic strain , is described by the isotropic model developed by Mazars (1984). The plastic process is described by means of a yield surface, inspired from Etse and Willam (1994) and modified by Crouch and Tahar (2000). In this approach, damage controls softening, while plasticity controls harding, in compression especially.

This model generates ill-posed mathematical problems due to the loss of ellipticity of the governing differential equations. Numerically, the results suffer from pathological sensitivity to the size and the orientation of the finite element mesh and the total energy dissipated by the fracture process tends to zero upon mesh refinement. Several nonlocal constitutive laws, which can be regarded as a remedy of the pathalogical mesh dependence, can be found in the literature. Whether they are in an integral form (Pijaudier-Cabot and Bažant 1987) or in a gradient form (Peerlings et al. 1996), a salient characteristic of both types is the presence of a characteristic length in the constitutive relation.

The aim of this paper is to extend the previous approach to a non local model in order to simulate properly concrete structure behaviour with mixed mode failure. The regularization technique, based on the implicit gradient definitions of the nonlocal strain tensor, is adopted to overcome the mathematical problems due to the softening constitutive law (damage part), while the plastic part remains local.

In this contribution, the constitutive law of the model is first presented. Then, the validation and the performance of the model is evaluated in some structural cases.

2 MODEL FORMULATION

The effective stress approach has been chosen for coupling plasticity and damage effects. The total stress $\boldsymbol{\sigma}$ is then a function of the damage variable D and of an effective stress $\boldsymbol{\sigma}'$ that solves the equation of a plastic yield surface

$$\boldsymbol{\sigma} = (1 - D)\boldsymbol{\sigma}' \tag{1}$$

2.1 *Plasticity*

Elastoplastic constitutive law is defined by the following set of equations in which the effective stress $\boldsymbol{\sigma}'$ has been substituted to the applied stress $\boldsymbol{\sigma}$:

$$\begin{aligned} \boldsymbol{\varepsilon} &= \boldsymbol{\varepsilon}^e + \boldsymbol{\varepsilon}^p \\ \boldsymbol{\sigma}' &= \boldsymbol{E}\boldsymbol{\varepsilon}^e \\ \dot{\boldsymbol{\varepsilon}}^p &= \dot{\lambda}\boldsymbol{m}\left(\boldsymbol{\sigma}', \boldsymbol{\kappa}\right) \\ \dot{\boldsymbol{\kappa}} &= \dot{\lambda}\boldsymbol{h}\left(\boldsymbol{\sigma}', \boldsymbol{\kappa}\right) \end{aligned} \tag{2}$$

where $\boldsymbol{\varepsilon}$, $\boldsymbol{\varepsilon}^e$ and $\boldsymbol{\varepsilon}^p$ are the total, elastic and plastic strains respectively, $\boldsymbol{E}$ is the elastic stiffness tensor, $\boldsymbol{m}$ is the flow vector, $\boldsymbol{\kappa}$ is the set of internal variables and $\boldsymbol{h}$ is the plastic modulus. The plastic multiplier $\dot{\lambda}$ is given by the loading-unloading criterion (Kuhn-Tucker form)

$$F\left(\boldsymbol{\sigma}', \boldsymbol{\kappa}\right) \leq 0, \quad \dot{\lambda} \geq 0, \quad F\left(\boldsymbol{\sigma}', \boldsymbol{\kappa}\right)\dot{\lambda} = 0, \tag{3}$$

where $F\left(\boldsymbol{\sigma}', \boldsymbol{\kappa}\right)$ is the yield function that defines the effective stress state. The plastic flow vector $\boldsymbol{m}$ is defined as (associated law)

$$\boldsymbol{m} = \frac{\partial F}{\partial \boldsymbol{\sigma}'} \tag{4}$$

The plastic yield surface, inspired from Etse and Willam (1994) and modified by Crouch and Tahar (2000), depends on four main functions $\bar{\rho}$ (effective stress invariant), $\hat{k}$ (hardening function), $\bar{\rho}_c$ (deviatoric parameter) and r (deviatoric shape function) (for more details, see (Jason et al. 2006))

$$F = \bar{\rho}^2\left(\boldsymbol{\sigma}'\right) - \frac{\hat{k}\left(\boldsymbol{\sigma}', k_h\right)\bar{\rho}_c\left(\boldsymbol{\sigma}'\right)}{r^2\left(\boldsymbol{\sigma}'\right)} \tag{5}$$

where k_h is the hardening variable given as a function of confinement:

$$\begin{aligned} \dot{k}_h &= \frac{\sqrt{\frac{2}{3}\varepsilon^p : \varepsilon^p}}{\zeta(\sigma')} \quad \text{if} \quad k_h < 1, \\ \dot{k}_h &= 0 \qquad\qquad\quad \text{if} \quad k_h = 1, \end{aligned} \tag{6}$$

where ζ depends on the first normalized invariant

$$\begin{aligned} \zeta &= -A_h + \sqrt{A_h^2 - B_h\bar{\xi} + C_h} \quad \text{if} \quad \bar{\xi} \leq 0, \\ \zeta &= -A_h + \sqrt{A_h^2 + C_h} \qquad\quad \text{if} \quad \bar{\xi} > 0, \end{aligned} \tag{7}$$

A_h,B_h,C_h are three model parameters. Note that equation (7) assumes that k_h ranges between 0 and 1. When $k_h = 1$, the yield surface becomes a limit surface with no hardening in pure elasto-plastic model. Combining equations (2) and (7) yields the following expression for the plastic modulus h:

$$\begin{aligned} h &= \frac{\sqrt{\frac{2}{3}\frac{\partial F}{\partial \sigma'} : \frac{\partial F}{\partial \sigma'}}}{\zeta(\sigma')} \quad \text{if} \quad k_h \leq 1, \\ h &= 0 \qquad\qquad\qquad\qquad\quad \text{if} \quad k_h = 1, \end{aligned} \tag{8}$$

The plastic part of the constitutive relation contains 10 parameters in which four parameters remains at a fixed value: $\alpha = 0.5$, $\gamma = 0.99$, $A_h = 7 \times 10^{-5}$ and $k_0 = 0.1$ (for more details, see (Jason et al. 2006)). Only two parameters r_c and r_t will be given in the applications where the others are taken as $p = 0.4$, $B_h = 2 \times 10^{-2}$, $C_h = 2 \times 10^{-6}$ and $A = -0.5$.

2.2 *Damage model*

Damage growth, controlled by elastic strain tensor, is governed by the following loading function:

$$g(\boldsymbol{\varepsilon}^e, k_d) = \varepsilon_{eq}(\boldsymbol{\varepsilon}^e) - k_d \tag{9}$$

where ε_{eq} is the equivalent strain. k_d initially equals the damage threshold ε_{D_0} and during the damage process equals the largest ever reached value of ε_{eq}. The evolution of damage is governed by the standard loading/unloading condition:

$$g(\boldsymbol{\varepsilon}^e, k_d) \leq 0, \quad \dot{k_d} \geq 0, \quad \dot{k_d}g(\boldsymbol{\varepsilon}^e, k_d) = 0 \tag{10}$$

For quasi-brittle materials such as concrete, the damage propagates much more easily under tension than under compression. Taking that into account, one possible choice is the so-called modified von Mises definition according to de Vree et al. (1995)

$$\begin{aligned} \varepsilon_{eq} &= \frac{k-1}{2k(1-2\nu)}I_1 \\ &+ \frac{1}{2k}\sqrt{\frac{(k-1)^2}{(1-2\nu)^2}I_1^2 + \frac{6k}{(1+\nu)^2}J_2} \end{aligned} \tag{11}$$

where I_1 is the first invariant of strain tensor, J_2 is the second deviatoric invariant of the strain tensor and k is the ratio between uniaxial compressive and tensile strengths. This model uses only one single damage function

$$D = 1 - \frac{1-A}{\varepsilon_{eq}} + \frac{A}{exp\left(B\left(\varepsilon_{eq} - \varepsilon_{D_0}\right)\right)} \tag{12}$$

where A and$B$ are two constant of the model. In this contribution, Mazars' definition of equivalent strain is used

$$\varepsilon_{eq} = \sqrt{\sum_{i=1}^{3}\left(\langle\varepsilon_i^e\rangle_+\right)^2} \tag{13}$$

where $\langle \varepsilon_i^e \rangle_+$ are the positive principal elastic strains. The damage variable D is determined as a linear combination of two damage variables D_t and D_c, that represent tensile damage and compressive damage respectively, by the help of two coefficients α_t and α_c computed from the elastic strain tensor and depending on the type of effective stress state:

$$D = \alpha_t D_t + \alpha_c D_c \tag{14}$$

$$D_{t,c} = 1 - \frac{1 - A_{t,c}}{\varepsilon_{eq}} + \frac{A_{t,c}}{exp\left(B_{t,c}\left(\varepsilon_{eq} - \varepsilon_{D_0}\right)\right)} \tag{15}$$

$$\alpha_{t,c} = \left(\sum_{i=1}^{3} \frac{\varepsilon_i^{t,c} \langle \varepsilon_i^e \rangle_+}{\varepsilon_{eq}} \right) \tag{16}$$

where A_t, B_t, A_c, B_c are four model parameters. ε^t and ε^c are the principal values of strains associated to the positive and negative effective stresses respectively.

The combination of plasticity and damage exhibits strain-softening and all the inherent difficulties attached to this specific material behavior, i.e., spurious strain localization and dependence of the energy dissipation on mesh refinement. To avoid this undesirable behaviour, the model may be regularized considering a nonlocal approach. In the present paper, a regularization technique, similar to that presented by Peerlings et al. (1996), is chosen. It is based on implicit gradient definition of the nonlocal strain tensor which is calculated for each component of the elastic strain tensor as:

$$\boldsymbol{\varepsilon}_{ij}^e = \bar{\boldsymbol{\varepsilon}}_{ij}^e - c\nabla^2 \bar{\boldsymbol{\varepsilon}}_{ij}^e \tag{17}$$

where ∇^2 is the Laplacian operator. The parameter c is of the dimension length squared and characterizes the non local interaction. This equation must be completed by the homogeneous Neumann boundary conditions

$$\nabla \bar{\boldsymbol{\varepsilon}}^e . n = 0 \tag{18}$$

with n the outward unit normal to the physical boundary. Now the local equivalent strain in equation (13) is replaced by its nonlocal counterpart:

$$\bar{\varepsilon}_{eq} = \sqrt{\sum_{i=1}^{3} \left(\langle \bar{\varepsilon}_i^e \rangle_+ \right)^2} \tag{19}$$

3 STRUCTURAL APPLICATION

3.1 *Bar under uniaxial tension*

The validation of the regularization technique introduced to the damage part of the model is illustrated by means of a tension bar with a defect in the middle. The bar length is $1\ m$ and the cross section is 2×2 cm^2. In simple tension tests, when the yield surface is reached, the effective response of the plastic damage constitutive law presented in this paper is perfectly plastic and no further damage can evolve due to a constant elastic strain. For this reason, the plastic process in this example is described by the Von Mises' model with linear hardening and no limit surface. The following parameters are used in this analysis: $E = 3.3 \times 10^{10}$ Pa, $\nu = 0.2$, $A_t = 0.9$, $B_t = 10000$, $\varepsilon_{D_0} = 10.5 \times 10^{-5}$, $\sigma_y = 3 \times 10^6$ Pa and $E_t = 1.1 \times 10^{10}$ Pa, where σ_y the yield stress and E_t the hardening modulus are the marerial properties for plastic part. Fig. 1 shows the damage distribution over the bar close to failure for a non local parameter *c* equal to 0.002 m^2.

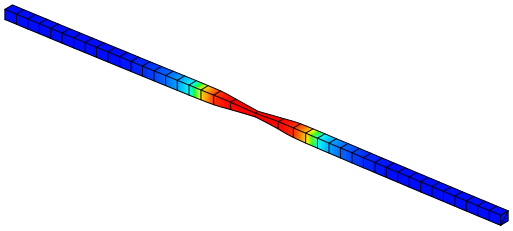

Figure 1: Development of damage in a tensile bar with a defect in the middle.

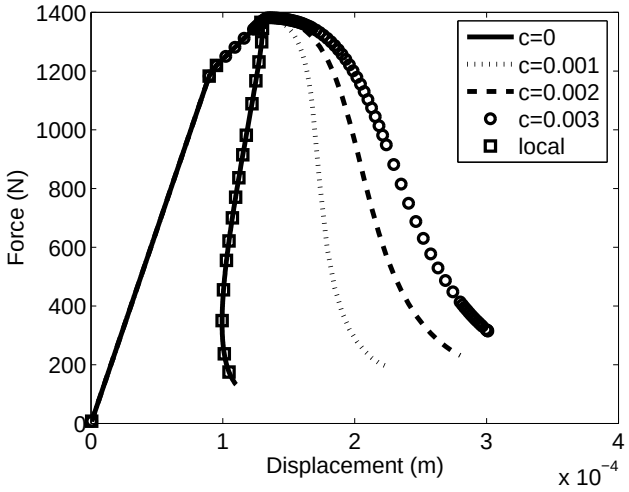

Figure 2: Load displacement responses for different internal lengths.

The properties of the plastic gradient damage model are assessed by carrying out the analysis with several values of the gradient parameter *c* and a fixed mesh of 80 pentagon elements. Fig. 2 and Fig. 3 show the load-displacement response and the profile of damage for several values of the internal length parameter *c*. As desired, both the ductility in the load-displacement response and the width of the final damage profile increase with the internal length while for *c*= 0 the response of the regularized version coincide with that of the local one where the damage is localized in the center.

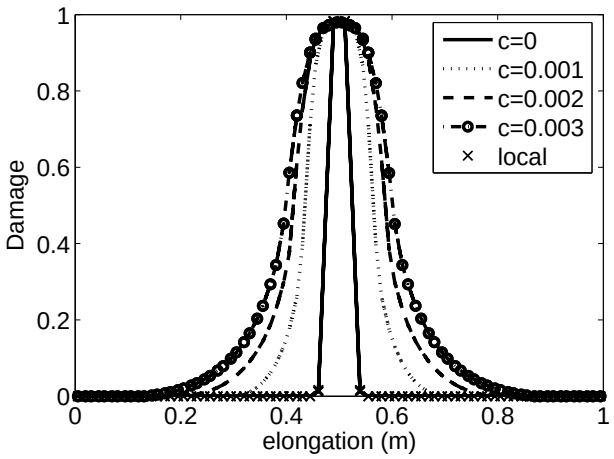

Figure 3: Damage profiles along the beam for different values of the internal length scale.

3.2 *Shear failure mode: local approach*

To demonstrate the abality and the performance of our constitutive law to predict correctly the failure mode in structural applications, the experimental behavior of reinforced concrete Continuous Deep Beam (reported by Asin (1992)) has been simulated. The specimen, whith a minimum amount of stirups, has been selected for numerical simulation. However, the vertical shear reinforcement was not taken into account to simplify the study. The material parameters for the concrete are: $E = 3.47 \times 10^{10}$ Pa, $\nu = 0.2$, $A_t = 1$, $A_c = 2.75$, $B_t = 13000$, $B_c = 2470$, $\varepsilon_{D_0} = 1 \times 10^{-4}$, $r_c = 120 \times 10^6$ Pa and $r_t = 11 \times 10^6$ Pa.

Moreover, a comparative numerical investigation has also been performed with two isotropic damage models in order to show advantages achieved by the introduction of plasticity into the damage formulation. The first one using the classical damage formulation defined by Mazars (1984) with the following parameters: $E = 3.47 \times 10^{10}$ Pa, $\nu = 0.2$, $A_t = 1$, $A_c = 2.75$, $B_t = 8000$, $B_c = 1768$, $\varepsilon_{D_0} = 1 \times 10^{-4}$, and the other one employing the modified von Mises definition of the equivalent strain according to de Vree et al. (1995) with the following parameters: $E = 3.47 \times 10^{10}$ Pa, $\nu = 0.2$, $A_t = 0.9$, $B_t = 8000$ and $\varepsilon_{D_0} = 1 \times 10^{-4}$. The reinforcement bars are modelled with a von Mises plasticity model with $E = 2.1 \times 10^{11}$ Pa, $\nu = 0.3$, $\sigma_Y = 5 \times 10^8$ Pa (yield stress), $Et = 4.5 \times 10^{10}$ Pa (tangent modulus).

The geometry and the loading setup are presented in Fig. 4 where the thickness is $0.15\ m$. Because of symmetry, only (the right) half of the specimen has been meshed with 3048 eight node cubic elements. With these geometry and parameters, the simulations are performed with the local approaches, since, using the nonlocal model presented in this paper would require a mesh small enough to take into account non local interaction and would reach computational limits due to the memory size of the calculation.

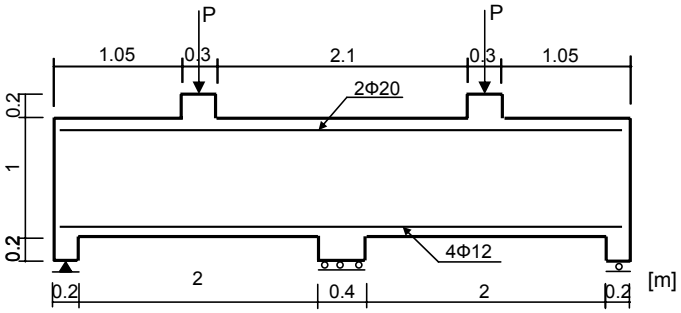

Figure 4: Geometry and loading setup of CDB.

A satisfactory agreement of the experimental and numerical results is observed. Fig. 5 provides a comparison of the experimental crack pattern with the numerical damage profile of the plastic damage model. As seen in the experiments, flexural damage band (mode I) starts first at midspan (stage A). Further load increase leads to the development of the flexural damage band and a propagation of damage (mode I & II) continues over the support (stage B), then a shear damage band (pure mode II) formed suddenly (stage C). Finally, failure occurs at the load introduction zone near the loading column (stage D). The ultimate failure load obtained experimentally was $1180\ kN$, the corresponding numerical value is $1285\ kN$, which is overestimated by 11%. Thus, the model can reproduce correctly the mode of failure and predict rather well the ultimate load.

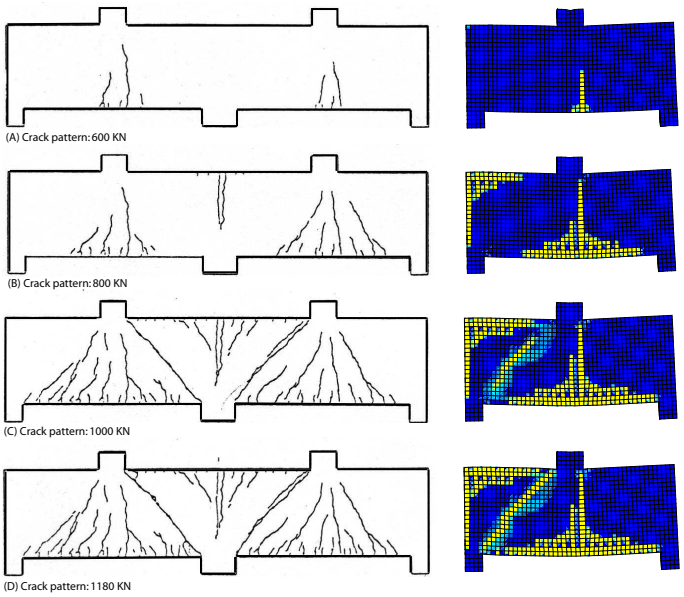

Figure 5: Developement of crack pattern in CDB; Experiment versus simulation with plastic damage model.

On the other hand, both damage models fail to reproduce the failure mode and the ultimate load observed during the test. Fig. 6 presents the crack pattern

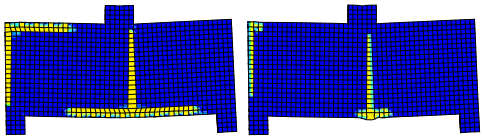

(a) (b)

Figure 6: Profiles of damage distribution in CDB with (a) Mazars' model and (b) modified von Mises' model.

obtained by the damage models, where only flexural cracks are formed. Fig. 7 compares the load deflection curves of the plastic damage and damage models. As expected, the peaks for the damage models are underestimated as the failure is in mode I. This strong difference is due to the fact that for Mazars' criteria is written only as a function of positive elastic strain (Eq. (13)) which means that it is only due to microcracks in mode I, while for the modified von Mises definition, the strength under biaxial tensile-compressive stress for concrete is overestimated which leads to overestimation of the shear resistance of the material in this model (see e.g. (Patzák and Jirázek 2004)).

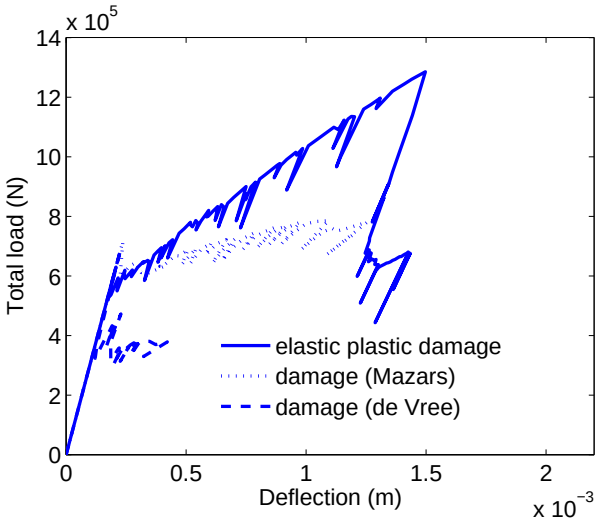

Figure 7: Load-deflection curves. Comparison between plastic damage model, Mazars' model and modified von Mises' model.

3.3 *Size effect in mixed mode tests*

Quasibrittle materials like concrete are charactarized by gradual softening in a fracture process zone (**FPZ**) that is independent and not negligeable compared to the structure size D. Hence, the response of geometrically similar specimens is not proportional and yield a material size effect (Bažant 1984). It can be explained by stress redistribution and the associated energy release due to the developement of large cracks or a large **FPZ** prior to failure. A complete explanation of the size effect can be found in the textbook by Bažant and Planas (1998). From the modelling viewpoint, the size effect can be described only with failure models that contain internal length which is related to the characteristic length of the material, i.e. the width of the **FPZ** (Mazars and Pijaudier-Cabot 1996).

The aim of this section is to highlight the existence of the size effect on the mixed mode failure as it is predicted by the plastic gradient enhanced damage formulation presented in this paper. Asymmetric four-point bending tests proposed by Gálvez et al. (1998) have been carried out on three notched geometrically similar specimens of different sizes, with relative dimension and loading setup shown in Fig. 8. The specimens with various height D of 75, 150 and 300 mm are referred to as small, medium and large respectively. The thickness b has been kept constant to 50 mm for all the specimens in order to keep the same initial structural stiffness. The model parameters used for the simulation of the three specimens are: $E = 3.8 \times 10^{10}$ Pa, $\nu = 0.2$, $A_t = 0.95$, $A_c = 2.45$, $B_t = 17200$, $B_c = 2900$, $\varepsilon_{D_0} = 7.3 \times 10^{-5}$, $r_c = 135 \times 10^6$ Pa and $r_t = 12.5 \times 10^6$ Pa. The gradient parameter has been taken as $c = 0.000123\ m^2$.

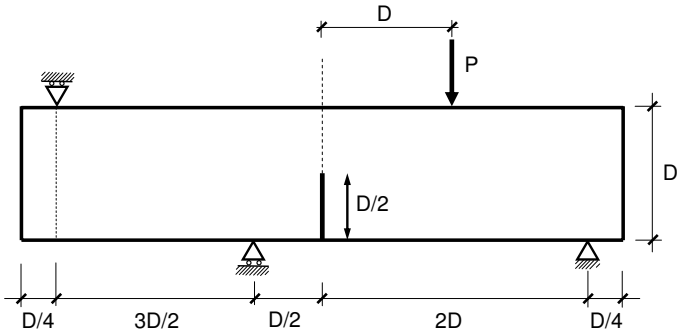

Figure 8: Geometry and loading setup for asymmetic four-point bending tests.

In order to avoid some possible mesh bias and ensure that the global energy dissipation in failure process is captured correctly, the size of an element in the process zone should be kept constant and small enough compared to the characteristic length.

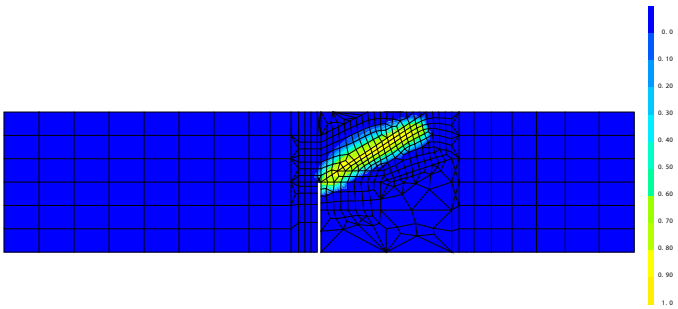

Figure 9: Profile of damage for small size specimen.

Fig. 10 shows the load deflection responses for the three different sizes. The nominal strength is obtained with the formula

$$\sigma_N = c_n \frac{P_u}{bD} \tag{20}$$

c_n is a constant depending on geometry which plays no role in size effect analysis. The ultimate loads P_u for the three sizes and its corresponding nominal strength are listed in the Table 1.

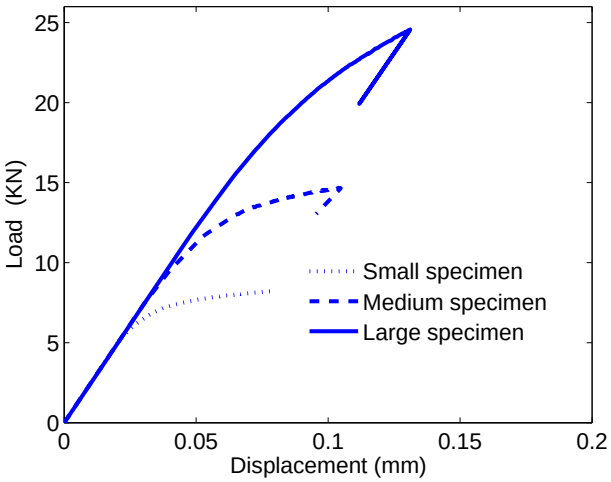

Figure 10: Load-displacement curves for small size specimen (D=75 mm), medium size specimen (D=150 mm) and large size specimen (D=300 mm).

Size	Depth D (mm)	Ultimate load P_u (kN)	Nominal strength σ_N (MPa)
small	75	8.213	2.19
medium	150	14.67	1.956
large	300	24.57	1.638

Table 1: Numerical results for three different sizes.

The numerical results are interpreted with the help of Bazant's size effect law (Bažant 1984).

$$\sigma_N = B f_t^{'} (1 + D/D_0)^{-1/2} \tag{21}$$

where B is a dimentionless geometry-dependent parameter, D_0 is a characteristic size and $f_t^{'}$ is the tensile strength of the material. $B f_t^{'} = 2.56$ MPa and $D_0 = 208.5$ mm have been conveniently determined by fitting process.

From this, the size effect law (equation (21)) is plotted in the form of logarithm of $\sigma_N / B f_t^{'}$ versus the logarithm of D/D_0 as shown in fig. 11. The size effect according to strength of material criterion is in this plot represented by a horizontal line and to linear elastic fracture mechanics (LEFM) is depicted by a line of

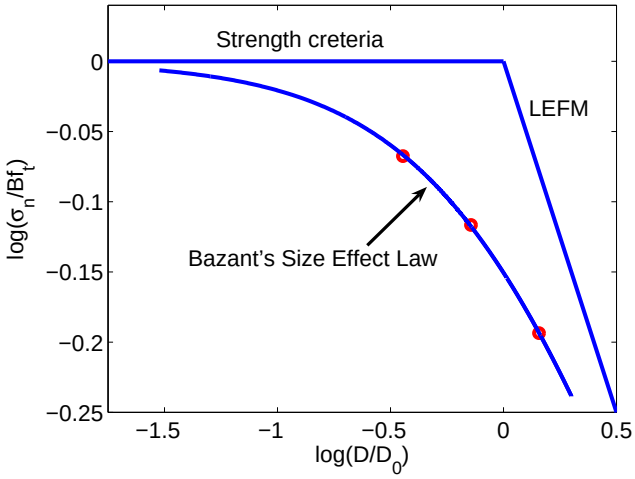

Figure 11: Size effect on nominal strength.

slope $-1/2$ where these two lines intersect at the abscissa $D = D_0$. Obviously, it can be seen that there is a pronounced size effect that is in a good agreement with Bazant's size effect relation. The larger the specimen, the lower the nominal strength. It is also observed that the plasticity plays more important role for the smaller specimen (the hardening variable k_h is more important as the specimen is smaller). On the other hand, for the larger specimen the developement of damage is dominant and its behavior is closer to linear elastic fracture mechanics and more different from a limit analysis solution.

4 CONCLUSION

In this work, the hardening plasticity is combined with a gradient enhanced damage formulation for modelling the structure behaviour with mixed mode failure. The example of tensile bar shows the effectivity of the regularization technique to overcome the mathematical problems due to the strain softening behaviour (damage part) where the damage distribution zone is controlled by a material heterogeneity parameter. Furthermore, the simulations of the Continuous Deep Beam show the improvements achieved by the coupled model compared to the damage models. The model predicts rather accurately the failure mode (e.g. mode II) and the ultimate load in complex structures.

Finally, the numerical simulations of three asymmetric four-point bending tests on notched specimens of different sizes show a dependence of the nominal strength on the specimen size. The larger the specimen, the lower the nominal strength. Thus, the nonlocal approach exhibits a size effect in mixed mode failure which is in a good agreement with Bazant's size effect relation.

REFERENCES

Asin, M. (1992). Behavior of statically interminate deep beams. In *Progress in Concrete research*, Volume 3, Delf University of technology, pp. 45–58.

Bažant, Z. P. (1984). Size effect in blunt fracture: concrete, rock, metal. *Journal of Engineering Mechanics 110*, 518–535.

Bažant, Z. P. and J. Planas (1998). *Fracture and Size Effect in Concrete and Other Quasi-Brittle Materials*. Boca Raton and London.

Crouch, R. and B. Tahar (2000). Application of a stress return algorithm for elasto-plastic hardening-softening models with high yeild surface curvature. In *Proceedings of European Congress on computational methods in Applied Sciences and Engineering*, Barcelona.

de Vree, J., W. Brekelmans, and A. van (1995). Comparison of nonlocal approaches in continuum damage mechanics. *Computers and Structures 55*, 581–588.

Etse, G. and K. Willam (1994). Fracture energy formulation for inelastic behavior of plain concrete. *Journal of Engineering Mechanics 106*(9), 1013–1203.

Gálvez, J., M. Elices, G. Guinea, and J. Planas (1998). Mixed mode fracture of concrete under proportional and nonproportional loading. *International Journal of Fracture 94*, 267–284.

Jason, L., A. Huerta, G. Pijaudier-Cabot, and S. Ghavamian (2006). An elastic plastic damage formulation for concrete: Application to elementary tests and comparison with an isotropic damage model. *Computer Methods in Applied Mechanics and Engineering 195*(52), 7077–7092.

Mazars, J. (1984). *Application de la mécanique de l'endommagement au comportement non linéaire et à la rupture de béton de structure*. Ph. D. thesis, Université Pierre et Marie Curie.

Mazars, J. and G. Pijaudier-Cabot (1996). From damage to fracture mechanics and conversely: a combined approach. *International Journal of Solids and Structures 33*, 3327–3342.

Patzák, B. and M. Jirázek (2004). Adaptivity resolution of the localized damage in quasi-brittle materials. *Journal of Engineering Mechanics 130*, 720–732.

Peerlings, R. H. J., R. de Borst, W. A. M. Brekelmans, and J. H. P. de Vree (1996). Gradient enhanced damage for quasi-brittle materials. *International Journal for Numerical Methods in Engineering 39*, 937–953.

Pijaudier-Cabot, G. and Z. Bažant (1987). Nonlocal damage theory. *Journal of Engineering Mechanics 113*, 1512–1533.